ELSEVIER

The Journal of Heart and Lung Transplantation
http://www.jhltonline.org

Early detection of cardiac allograft vasculopathy using highly automated 3-dimensional optical coherence tomography analysis

Michal Pazdernik, MD,[a,b] Zhi Chen, PhD,[c] Helena Bedanova, MD, PhD,[d] Josef Kautzner, MD, PhD,[a] Vojtech Melenovsky, MD, PhD,[a] Vladimir Karmazin, MD,[a] Ivan Malek, MD, PhD,[a] Ales Tomasek, MD,[d] Eva Ozabalova, MD,[e] Jan Krejci, MD, PhD,[e] Janka Franekova, MD, PhD,[f] Andreas Wahle, PhD,[c] Honghai Zhang, PhD,[c] Tomas Kovarnik, MD, PhD,[a,g] and Milan Sonka, PhD[c]

From the [a]Department of Cardiology, Institute for Clinical and Experimental Medicine, Prague, Czech Republic; [b]Department of Cardiology, Second Medical School, Charles University, University Hospital Motol, Prague, Czech Republic; [c]Iowa Institute for Biomedical Imaging, University of Iowa, Iowa City, Iowa, USA; [d]Cardiovascular and Transplantation Surgery, Brno, Czech Republic; [e]Department of Cardiovascular Diseases, St. Anne's University Hospital and Masaryk University, Brno, Czech Republic; [f]Department of Laboratory Methods, Institute for Clinical and Experimental Medicine, Prague, Czech Republic; and the [g]Second Department of Internal Medicine, Department of Cardiovascular Medicine, First Faculty of Medicine, Charles University in Prague and General University Hospital in Prague, Prague, Czech Republic.

KEYWORDS:
cardiac allograft vasculopathy;
OCT;
intimal thickness;
cholesterol;
rapid progression

BACKGROUND: Optical coherence tomography (OCT)–based studies of cardiac allograft vasculopathy (CAV) published thus far have focused mainly on frame-based qualitative analysis of the vascular wall. Full capabilities of this inherently 3-dimensional (3D) imaging modality to quantify CAV have not been fully exploited.

METHODS: Coronary OCT imaging was performed at 1 month and 12 months after heart transplant (HTx) during routine surveillance cardiac catheterization. Both baseline and follow-up OCT examinations were analyzed using proprietary, highly automated 3D graph-based optimal segmentation software. Automatically identified borders were efficiently adjudicated using our "just-enough-interaction" graph-based segmentation approach that allows to efficiently correct local and regional segmentation errors without slice-by-slice retracing of borders.

RESULTS: A total of 50 patients with paired baseline and follow-up OCT studies were included. After registration of baseline and follow-up pullbacks, a total of 356 ± 89 frames were analyzed per patient. During the first post-transplant year, significant reduction in the mean luminal area ($p = 0.028$) and progression in mean intimal thickness ($p = 0.001$) were observed. Proximal parts of imaged coronary arteries were affected more than distal parts ($p < 0.001$). High levels of LDL cholesterol ($p = 0.02$) and total cholesterol ($p = 0.031$) in the first month after HTx were the main factors associated with early CAV development.

CONCLUSIONS: Our novel, highly automated 3D OCT image analysis method for analyzing intimal and medial thickness in HTx recipients provides fast, accurate, and highly detailed quantitative data on early

Reprint requests: Michal Pazdernik, MD, FESC, Institute for Clinical and Experimental Medicine, Prague, 140 21, Czech Republic. Telephone: 420 236052985.

E-mail address: michal.pazdernik@email.cz

https://doi.org/10.1016/j.healun.2018.04.002

CAV changes, which are characterized by significant luminal reduction and intimal thickness progression as early as within the first 12 months after HTx.
J Heart Lung Transplant 2018;37:992–1000

Cardiac allograft vasculopathy (CAV) is a major cause of mortality in heart transplant (HTx) patients.[1,2] In its early stages the disease affects the intima but later manifests as typical atherosclerosis characterized by vulnerable plaques.[3] Optical coherence tomography (OCT) enables the thin intimal layer to be clearly differentiated from the tunica media, a crucial factor in determining early progression of CAV. OCT imaging can reveal rapid progression of CAV as early as during the first year after HTx.[4] Early diagnosis is of crucial importance as further progression of the disease can be managed using specific medical approaches.[5,6] Studies published thus far have yet to fully utilize the capabilities of 3-dimensional (3D) OCT for early quantitative analysis of CAV development, largely because manual coronary layer segmentation is a time-consuming process.[7–10] Our aim was to design a novel, highly automated image analysis method for assessing intimal and medial thickness (IT, MT) using OCT images from HTx patients.

Methods

Patients

Between October 2014 and December 2015, 50 subjects from the Heart Center at IKEM, Prague, Czech Republic, and from the Center of Cardiovascular and Transplantation Surgery, Brno, Czech Republic, were enrolled. The study (Clinical Trial NCT02503566) complied with the Declaration of Helsinki and was approved by the respective ethics committees. All HTx recipients ≥18 years of age were considered eligible for inclusion in the study provided they were able and willing to give their informed consent. Exclusion criteria were renal insufficiency Stage ≥IV (glomerular filtration 30 ml/min), unfavorable post-transplant clinical conditions such as episodes of severe rejection or nosocomial sepsis with prolonged antibiotic treatment during the first month, ongoing need for circulatory support using a ventricular assist device, and acute allograft failure.

OCT method

The reported method of OCT acquisition and analysis consists of the following main steps:

1. Image acquisition including vessel wiring (catheterization lab, 5 minutes).
2. Expert definition of excluded angular regions (computer-assisted, 1 hour per pullback).
3. One- to 12-month pullback registration (computer-assisted, 10 to 15 minutes).
4. Multilayer 3D segmentation (automated, 20 seconds).
5. "Just-enough-interaction" (JEI) adjustment (computer-assisted, 2 to 15 minutes).
6. Quantitative analysis (automated, immediate).

Image acquisition

Coronary OCT imaging was performed at 1 month (1M) and 12 months (12M) after HTx as part of routine surveillance cardiac catheterization with a commercial intracoronary OCT system (Ilumien/Dragonfly Optis; St. Jude Medical, St. Paul, MN). A 54-mm-long segment of each HTx patient's left anterior descending (LAD) artery, located within a proximal 100-mm segment, was imaged at 1M and 12M using automated pullback at 18 mm/s and 10 frames/mm. When the LAD exhibited unfavorable anatomic characteristics (small caliber, extreme tortuosity, muscle bridge), 100-mm proximal segments of the left circumflex (LCx) or the right coronary artery (RCA) were imaged. The baseline and follow-up OCT-imaged segments mutually overlapped.

Image interpretation

For each frame of all OCT pullbacks, luminal, intimal, and medial surfaces were automatically segmented using a fully 3D LOGISMOS graph-based approach developed at the University of Iowa (Figure 1).[11,12] Boundaries were identified as OCT brightness changes showing tissue interfaces between adjacent wall layers. Automatically identified borders were efficiently edited using our JEI method adapted for the OCT segmentation environment.[13,14] This technique allows segmentation errors to be corrected in a 3D fashion on a regional basis, as opposed to contour-by-contour/frame-by-frame manual retracing (Figure 2). This highly accurate multilayer model facilitated quantitative CAV analysis of every frame of the imaged vessel for both baseline and follow-up image pullbacks. After identifying corresponding vascular landmarks, baseline and follow-up pullback pairs were co-registered, facilitating location-specific and fully 3-dimensional comparisons of layer-based changes using quantitative indices.

Quantitative descriptors

Branches and ambiguous areas of the wall were excluded from the analysis according to the consensus of 2 expert cardiologists. Full frames were only excluded when appearing in 1 but not in the other of the 2 registered pullbacks. Branch locations were used to calculate distances from the nearest branch.

The luminal, intimal, and medial layers for each frame were segmented and analyzed to obtain average thickness and area. The intima-to-media (I/M) ratio was calculated by dividing the average intimal thickness (IT) by the average medial thickness (MT) for each frame of the analyzed pullbacks. Global intimal thickening, $\Delta IT = IT_{12M} - IT_{1M}$, was determined as the average difference between IT at 1M and 12M at all co-registered vessel wall locations. Maximal segmental intimal thickening, $\Delta SIT = \max\{SIT_{12M} - SIT_{1M}\}$, was determined by comparing all 3-mm-long, 90° wedges of the vessel wall, with SIT_{12M} and SIT_{1M} as the average intimal thicknesses in the respective registered wedge segments.

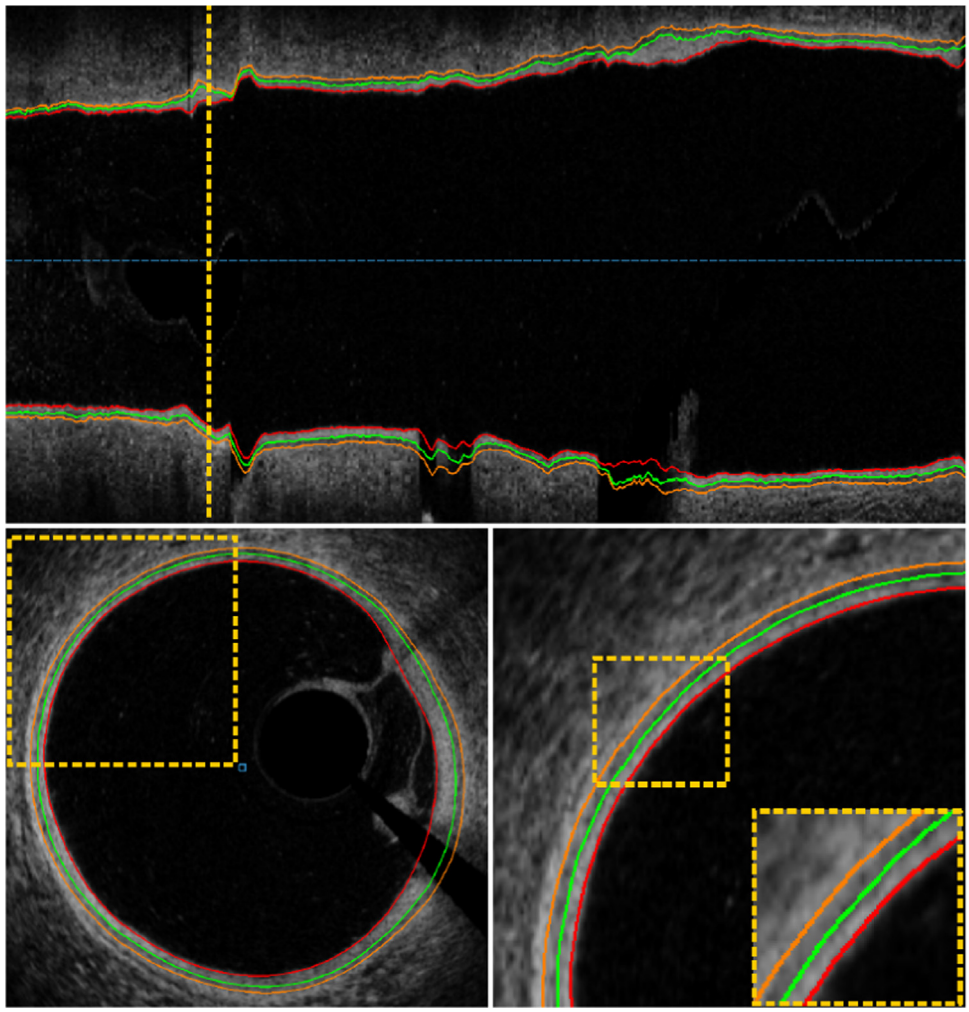

Figure 1 Automatic 3D segmentation of the coronary wall. LOGISMOS simultaneous 4-surface 3D segmentation of luminal (red), outer intimal (green), and outer medial (orange) surfaces of coronary wall layers from a heart transplant patient. Cross-sectional images show locations in a vertical line.

Full 3D analysis of the vessel wall enabled the development of quantitative focal wall disease descriptors to reflect the presence and appearance of regions with above-threshold donor-associated intimal thickness and to assess relationships between these indices and 1M to 12M intimal thickening:

1. Donor-associated intimal thickness load (%)—percentage of wall surface with local IT $>$ x.
2. Size of the largest region exhibiting increased IT (mm^2)—largest contiguous region with local IT $>$ y.
3. Number of large regions exhibiting increased IT—number of contiguous regions larger than a pre-specified area with local IT $>$ y.

Qualitative descriptors

Based on recent work by Clemmensen et al,[15] the vessel disease phenotype was estimated by qualitative analysis and characterized as 1 of 4 vessel wall phenotypes: (a) normal; (b) thrombofibrotic (2 or more areas with layered fibrotic plaque); (c) atherosclerotic (1 or more area[s] with lipid plaque); and (d) mixed atherosclerotic and thrombofibrotic. Relationships between vessel wall phenotypes at 1M and either global ΔIT or segmental ΔSIT intimal thickening were quantified.

Comparison between JEI computer and manual analysis

Segmentation performance was assessed in 38 OCT pullbacks from 20 HTx patients. Two experts manually defined the independent standard in a subset of 394 image frames (~10 frames/pullback) and the interobserver variability was determined. The accuracy of the computer analysis (automated segmentation followed by JEI) was reported using signed errors of intimal and medial thickness and compared with interobserver variability.

Inter- and intraobserver reproducibility

To evaluate interobserver variability, 13,918 frames from 15 randomly chosen pullbacks were analyzed by 2 experts using automated segmentation followed by JEI expert-guided refinement. For intraobserver variability, 12,706 frames from another set of 15 randomly chosen pullbacks were analyzed by the same experts using automated segmentation, followed by JEI refinement. Four months elapsed between the 2 rounds of JEI analysis to ensure their independence.

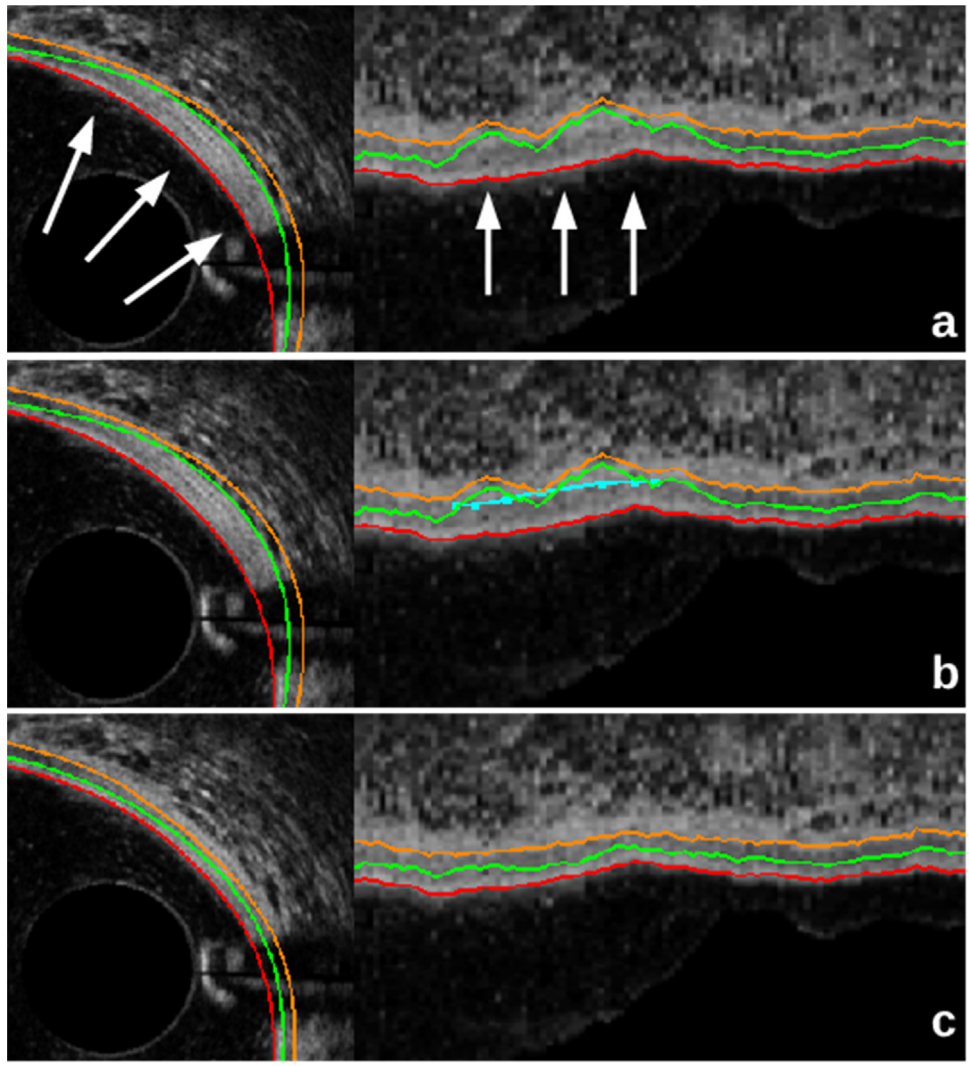

Figure 2 "Just-enough-interaction" (JEI) tool enabling manual correction of automatic wall layer analysis. (a) Automated multilayer segmentation showing an inaccuracy (arrows) due to a layer-like microstructure coming from the adventitia (the outermost surface as well as cross-sectional and axial views in 3D volume are shown). (b) User-defined desired location (blue points) of the outer-intimal surface (orange line). (c) Recomputed surfaces after JEI. All surfaces were corrected simultaneously and in 3D, even though only a few points in one 2D plane were specified by the user.

Statistical analysis

Numerical variables are described as mean ± standard deviation or as median and interquartile range (IQR), as appropriate. Categorical variables, presented as count and percentage, were compared using Fisher's exact test. To evaluate computer-analysis reproducibility, layer thickness measurements were compared using the paired *t*-test. To investigate the association between changes in IT and continuous variables, such as branch distances, mixed-effect analysis (with the patient as the random effect) was used to correct the clustering of multiple frames among patients. To evaluate risk factors among progression and non-progression patients, the cohort was divided into tertiles based on ΔIT at 12M (non-Gaussian distribution). The 33% tertile of patients with lowest IT progression and the 33% tertile with highest IT progression were compared. To evaluate associations of focal wall disease descriptors with ΔIT, linear regression analysis was used. Associations between vessel wall phenotypes and ΔIT (ΔSIT) utilized 1-way analysis of variance (ANOVA) after logarithmic normalization. Bonferroni's correction was applied as appropriate. The R environment (R Foundation for Statistical Computing, Vienna, Austria) was employed for statistical computing and $p < 0.05$ was considered statistically significant.

Results

Patients' characteristics are summarized in Table 1. In this population, 41 LAD, 3 LCx, and 6 RCA arteries were analyzed.

Cohort analysis

In the 50 1M / 12M pairs of registered OCT pullbacks, the median analyzable angular range was 250° (IQR 180° to 351°) per frame. No full frames were excluded after image registration and the average overlapping pullback length was 35.6 ± 8.9 mm. A total of 356 ± 89 registered frame pairs were analyzed per patient, resulting in an average co-registered intimal surface area of 380 ± 97 mm^2 per vessel

Table 1 Patients' Characteristics

	Patient cohort ($n = 50$)
Age (years)	50.9 (± 12.7)
Men	76% (38)
BMI 1M/12M	26.3 (± 4.1) / 28.5 (± 4.2)
Arterial hypertension before HTx	34% (17)
Hyperlipidemia before HTx	46% (23)
Diabetes mellitus before HTx	24% (12)
History of smoking	58% (29)
Ischemic cardiomyopathy before HTx	26% (13)
Donor age (years)	42.3 (± 12.1)
Donor gender (men)	60% (30)
CMV infection	18% (9)
Cold ischemia time (minutes)	125 (± 50.2)
Explosive brain death	66% (33)
Rejection mild	74% (37)
Rejection severe	6% (3)
Humoral rejection	2% (1)
LV ejection fraction (%) 1M / 12M	61 (± 4.6) / 62 (± 4.9)
Aspirin 1M / 12M	54% (27) / 68% (34)
Statin 1M / 12M	76% (38) / 84% (42)
Steroids 1M / 12M	100% (50) / 86% (43)
Tacrolimus 1M / 12M	100% (50) / 98% (49)
Cyclosporine 1M / 12M	0% (0) / 2% (1)
mTOR inhibitor (everolimus) 1M / 12M	0% (0) / 10% (5)
Mycophenolate mofetil 1M / 12M	100% (50) / 84% (42)

Data expressed as percent (n) or mean (± standard deviation). 1M, 1 month; 12M, 12 months; BMI, body mass index; CMV, cytomegalovirus; HTx, heart transplant; LV, left ventricle; mTOR, mechanistic target of rapamycin.

pullback; local descriptors were available for over 25,000 co-registered wall locations per pullback, on average.

Quantitative descriptive OCT characteristics showing CAV progression within 12 months after HTx are shown in Table 2. During the first post-transplant year, we observed a significant reduction in mean luminal area ($p = 0.028$) and a progression in mean intimal thickness ($p = 0.001$). Mean medial thickness remained unchanged during the first post-HTx year ($p = 0.866$). Our results show rapid manifestation of intimal thickening in some patients during the first year, whereas intimal thickness remained unchanged in other patients (Figure 3).The cohort was divided by tertiles of intimal thickening (33%, 66%) into 3 groups. In the lower group (33%), there was no significant change in intimal thickness between baseline and follow-up (the hypothesis that values differed was not supported at a significance level of $p = 0.895$), whereas, in the higher group (33%), there was a statistically significant change in intimal thickness ($p < 0.001$). According to tertile analysis of patient-based mean intimal thickness, among all the investigated donor-related characteristics and non-immunologic risk factors, the main factors associated with early CAV development were: (1) patient age ($p = 0.047$); and (2) high levels of both low-density lipoprotein (LDL) cholesterol ($p = 0.022$) and total cholesterol ($p = 0.034$) in the first month after HTx (Table 3).

According to mixed-effect analysis, absolute intimal thickness progression (in microns) was positively associated with vessel location (distance [in millimeters] from distal to proximal); $\beta = 32.9$, $p < 0.001$. This finding was further supported by comparative results of the most distal and proximal 5-mm segments (Figure 4). To offset the possible effects of a tapering vessel shape, relative intimal thickness progression (in percent), which is calculated as the absolute intimal thickness progression divided by the baseline luminal size, was found to be positively associated with vessel location (from distal to proximal); $\beta = 7.0$, $p < 0.001$.

Frame-based intimal thickness progression from 1M to 12M was not significantly associated with distance from the closest branch ($p = 0.46$). However, as shown in Figure 5, the frame of maximal intimal thickness progression over the whole pullback tended to be in close proximity to a coronary side-branch, regardless of spatial orientation (proximal or distal to bifurcation).To study the impact of donor disease on CAV development, each 1M / 12M pair measurement and comparison was based on analysis of the registered wall locations. When assessing the relationship between focal wall disease descriptors and ΔIT, 2 of the 3 indices exhibited statistically significant correlations (thresholds determined as maximizing the studied relationships). This suggests that: (1) the overall relative load of thickened intima at 1M and (2) the spatial distribution of large contiguous regions with thickened intima are the driving factors of early intimal thickening rather than the size of the single largest contiguous region:

- Donor-associated intimal thickness load ($x = 0.08$ mm) vs ΔIT; $R = 0.34$, $p = 0.016$.
- Size of the largest region exhibiting increased IT ($y = 0.20$ mm) vs ΔIT; no statistical significance (slope not significantly different from 0).
- Number of large regions exhibiting increased IT vs ΔIT ($y = 0.20$ mm, area = 10 mm^2); $R = 0.55$, $p < 0.001$.

Based on qualitative characterization of vessel wall phenotypes at 1M, 21 (42%) of the vessels studied were

Table 2 Optical Coherence Tomography Findings

	1M after HTx	12M after HTx	Change from 1M to 12M	p-value
Mean luminal area (mm^2)	8.7 ± 2.4	7.6 ± 2.3	−1.0 ± 1.6	0.028
Mean intimal thickness (μm)	105.3 ± 37	133.8 ± 48.8	28.4 ± 28.0	0.001
Mean medial thickness (μm)	81.9 ± 20.2	81.2 ± 18.8	−0.7 ± 11.2	0.866
Mean intimal/medial ratio	1.4 ± 0.3	1.7 ± 0.4	0.4 ± 0.3	0.005

Data expressed as mean ± standard deviation. 1M, 1 month; 12M, 12 months; HTx, heart transplant.

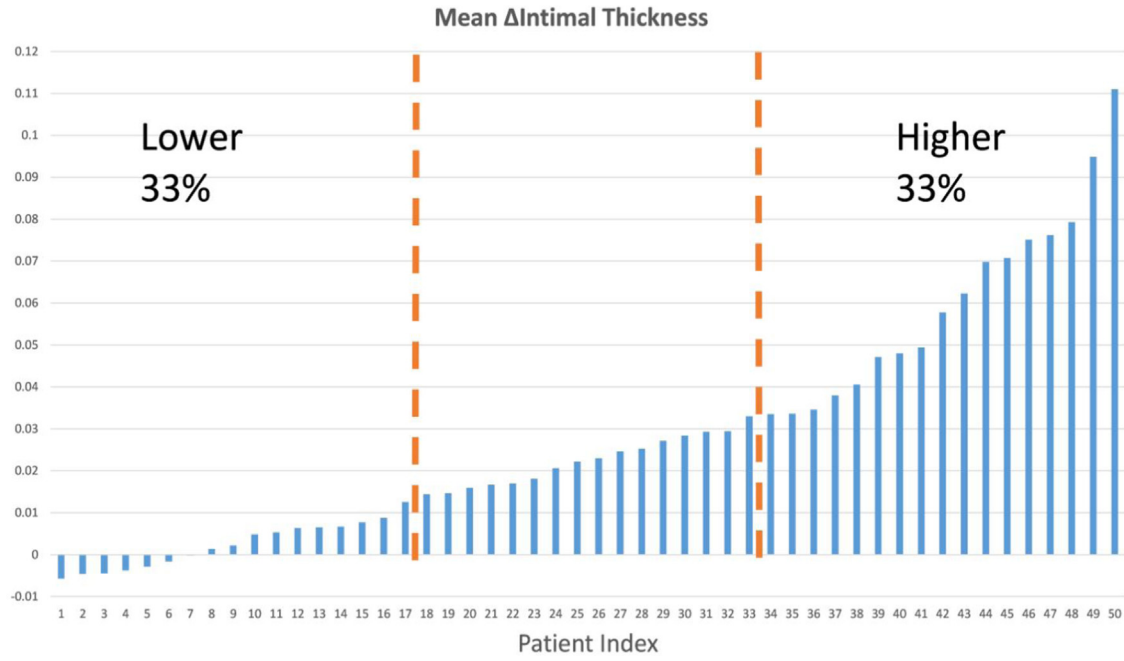

Figure 3 Mean intimal thickness progression (in millimeters) for an entire pullback in 50 consecutive patients. Patients indexed by mean intimal thickness progression within 12 months after heart transplant.

assigned a normal phenotype, 0 (%) a thrombofibrotic phenotype, 15 (30%) an atherosclerotic phenotype, and 14 (28%) a mixed atherosclerotic and thrombofibrotic phenotype. None of the phenotypes were associated with global intimal thickening ΔIT at 12M (p = not statistically significant [NS]). However, the represented phenotype groups showed positive associations with ΔSIT at 12M ($p = 0.033$, $\Delta SIT_{normal} = 23.7 \pm 23.9$ μm, $\Delta SIT_{athero} = 28.9 \pm 25.9$ μm, $\Delta SIT_{mixed} = 31.4 \pm 34.9$ μm), which suggests that the more complicated lesions increased the rate of segmental

Table 3 Predictive Factors of Cardiac Allograft Vasculopathy Progression

	Non-progression (lower 33%) ($n = 17$)	Progression (higher 33%) ($n = 17$)	p-value
Patient age (years)	55.94 ± 10.32	47.71 ± 12.79	0.047
Men (%)	88%	71%	0.398
Arterial hypertension before HTx (%)	41%	24%	0.465
Hyperlipidemia before HTx (%)	59%	35%	0.303
Diabetes mellitus before HTx (%)	29%	24%	1.00
Active smoking before HTx (%)	71%	47%	0.296
History of ischemic cardiomyopathy (%)	35%	18%	0.438
Donor age	41.88 ± 12.21	45.82 ± 12.39	0.357
Donor gender (men) (%)	82%	53%	0.141
Cold ischemia time (min)	119.47 ± 67.22	126.47 ± 47.71	0.729
Explosive brain death (%)	71%	53%	0.481
VAD before HTx (%)	35%	12%	0.225
Rejection mild (%)	71%	88%	0.398
Rejection severe (%)	6%	29%	0.175
Humoral rejection (%)	NA	NA	NA
CMV infection (%)	12%	18%	1
BMI (kg/m^2) 1M / 12M	27.39 ± 2.94 / 29.18 ± 3.71	25.84 ± 5.63 / 27.68 ± 5.08	0.323 / 0.334
Total cholesterol (mmol/liter) 1M / 12M	4.43 ± 10.99 / 4.19 ± 1.06	5.31 ± 1.31 / 4.41 ± 1.19	0.034 / 0.570
HDL cholesterol (mmol/liter) 1M / 12M	1.54 ± 0.35 / 1.07 ± 0.33	1.52 ± 0.44 / 1.29 ± 0.69	0.851 / 0.243
LDL cholesterol (mmol/liter) 1M / 12M	2.23 ± 0.71/2.24 ± 0.73	2.96 ± 1.02 / 2.35 ± 0.66	0.022 / 0.646
TAG (mmol/liter) 1M / 12M	1.44 ± 0.55/ 2.04 ± 1.23	1.88 ± 0.83 / 2.21 ± 1.83	0.078 / 0.760
HbA_{1C} (mmol/mol) 1M / 12M	42.65 ± 6.78 / 55.47 ± 27.47	41.56 ± 8.29 / 47.87 ± 17.36	0.685 / 0.374
Plasma glucose (mmol/liter) 1M / 12M	5.91 ± 2.13 / 8.08 ± 3.87	5.19 ± 1.13 / 6.61 ± 2.35	0.232 / 0.189

Data expressed as mean ± standard deviation or percent. The patient cohort was divided into tertiles based on intimal thickness progression within 12 months after heart transplant. The 33% tertile of patients with lowest intimal thickness progression was compared with the 33% tertile with highest IT progression for risk factors. 1M, 1 month; 12M, 12 months; BMI, body mass index; CMV, cytomegalovirus; HbA_{1C}, glycated hemoglobin; HDL, high-density lipoprotein; HTx, heart transplant; LDL, low-density lipoprotein; NA, not available; TAG, triacylglycerols; VAD, ventricular assist device.

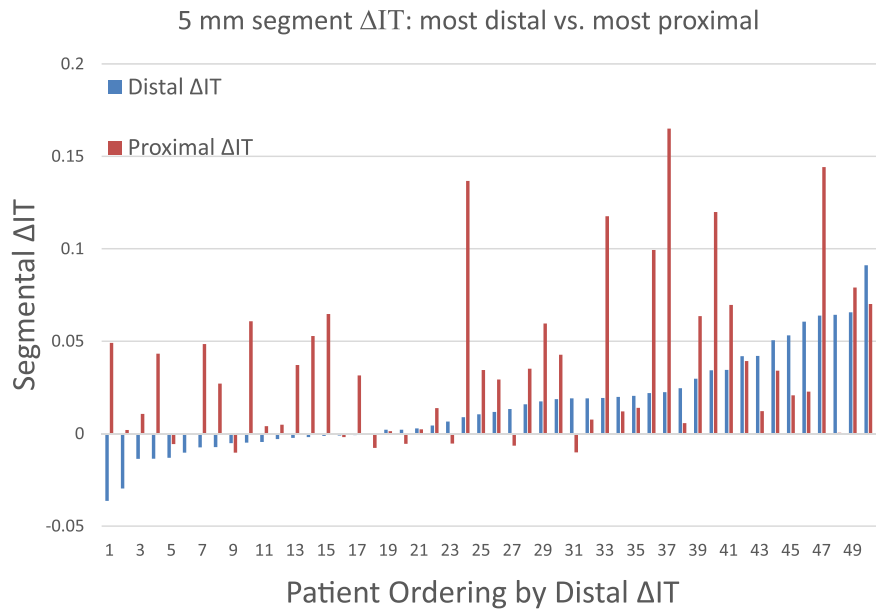

Figure 4 Progression of intimal thickness according to coronary artery location (proximal vs distal) in 50 consecutive patients within 12 months after heart transplant.

(or regional) rather than global (diffuse) intimal thickening at 12M.

Comparison between JEI computer and manual analysis

Based on computer analysis, signed errors of intimal and medial layer thickness were 0.4 ± 27.1 μm and 8.1 ± 12.2 μm, respectively. Interobserver variability using the same measurements was 3.6 ± 9.7 μm and –3.2 ± 12.6 μm. Direct regression analysis using manual and JEI computer measurements for intimal and medial thickness revealed that the indices obtained correlated with both IT and MT measurements ($R^2 = 0.99$, $p < 0.001$).

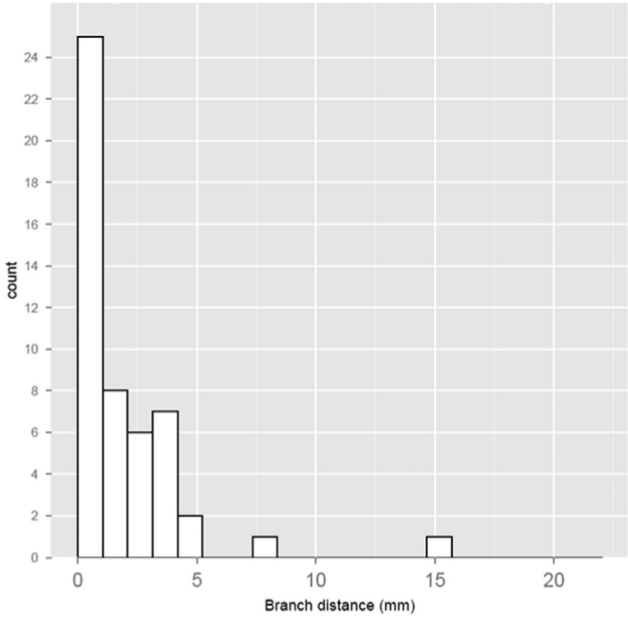

Figure 5 Histogram showing branch distances of all frames with maximal intimal thickness (MIT) progression. MIT progression related to branch distance in 50 patients.

Interobserver reproducibility of JEI computer analysis

The average signed (unsigned) surface-positioning difference between intimal layer surfaces was 0.37 ± 10.05 μm (4.22 ± 9.13 μm), whereas the average signed (unsigned) medial-layer surface-positioning difference was 1.49 ± 10.85 μm (4.32 ± 10.06 μm). Mixed-effect analysis showed that the 2 intimal–medial surface segmentations were not statistically significantly different from each other ($p = 0.92$, $p = 0.68$).

Intraobserver reproducibility of JEI computer analysis

The average signed (unsigned) surface-positioning difference between intimal layer surfaces was 1.77 ± 11.05 μm (5.74 ± 9.61 μm), whereas the average signed (unsigned) surface-positioning difference between medial layer surfaces was 1.77 ± 11.17 μm (5.66 ± 9.79 μm). Mixed-effect analysis showed that the 2 intimal–medial surface segmentations were not statistically significantly different from each other ($p = 0.61$, $p = 0.62$).

Discussion

The principal findings of this OCT study can be summarized as follows: (1) the reported approach for highly automated 3D OCT segmentation analysis provided the most sensitive quantitative OCT assessment of early CAV to date; (2) coronary artery changes after HTx showed significant luminal reduction and intimal thickness progression in a substantial proportion of patients; (3) proximal parts of

coronary arteries were affected more than distal parts; (4) increased levels of LDL and total cholesterol were the main risk factors for rapid intimal thickening; and (5) vessel wall phenotypes showed regional rather than global impact on intimal thickening.

Although prevention and treatment of acute transplant rejection have improved greatly in recent years, CAV still curtails the long-term survival of HTx patients. The limited preventive measures currently available include the treatment of co-morbidities (hypertension, diabetes mellitus, hypercholesterolemia), smoking cessation, prevention of cytomegalovirus (CMV) infection, avoiding acute cellular or humoral rejection, and the administration of mechanistic target-of-rapamycin (mTOR) inhibitor immunosuppressants.[1,16,17] Matsuo et al reported that sirolimus, in comparison with continued calcineurin inhibitor therapy, attenuated plaque progression in recipients with early conversion.[5] Therefore, early diagnosis is essential for preventing CAV-related allograft failure and subsequent need for re-transplantation.

OCT has demonstrated higher sensitivity than intravascular ultrasound (IVUS) with regard to early detection of CAV, attributable to its superior resolution of ≤10 μm, which is ≈10× higher than that of IVUS.[18] The OCT-based studies published thus far have focused mainly on qualitative analysis of CAV.[19–21] Furthermore, previous quantitative descriptions of CAV changes have not fully exploited the capabilities of 3D OCT, with usually only tens of available frames being analyzed.[7,8] A fast and highly automated method for full 3D intimal and medial measurements was reported. After registering the overlapping baseline and follow-up pullbacks, 356 ± 89 frames were analyzed per pullback. This approach is the most detailed quantitative OCT method available for assessing early changes in cardiac vasculature.

We observed rapid intimal thickening in the upper tertile of our patient cohort in agreement with previous studies that reported significant early CAV formation during the first year after HTx.[4,15] Moreover, we proved that a more diffuse pattern of donor-transferred disease, represented in our 3D analysis by the quantitative descriptors of intimal thickness load and the number of large regions with increased IT at 1M, was associated with early intimal thickening. With respect to vessel phenotype, coronary arteries with transferred atherosclerosis or more complicated mixed lesions were associated with more profound regional intimal thickening at 12M.

Once such patients are identified, patient-specific management may include adding the mTOR inhibitor everolimus. In addition, blood pressure and glycemia are strictly controlled, whereas statin doses are optimized after assessing CK-MB levels when required. Moreover, such patients may be scheduled for annually repeated invasive diagnostics.[22]

In agreement with findings by Dong et al,[7] our results suggest that proximal parts of imaged coronary vessels are affected more than distal parts. Earlier IVUS studies have shown that vascular branching sites are predisposing locations not only for donor-related atherosclerosis but also for the progression of intimal hyperplasia.[23] Intimal thickness progression in our patients was not significantly associated with distance from the closest branch, but the maximal intimal thickness progression for all pullbacks tended to be located in close proximity to coronary branches. These findings suggest that flow- and pressure-mediated wall shear stress is an important factor affecting focal progression of CAV beyond immunologic, metabolic, and infectious influences.[23]

A variety of CAV risk factors have been identified in recent years.[24–28] In our cohort, we observed that rapid intimal thickening was associated with increased levels of LDL cholesterol (regression slope $p = 0.022$) and total cholesterol ($p = 0.034$) early after HTx, but not associated with statin dose ($p =$ NS). Hyperlipidemia occurs in 60% to 83% of HTx recipients treated with conventional immunosuppressive therapy.[29,30] Lipid-lowering treatment using statins is one of the few therapeutic approaches capable of reducing both the development and progression of allograft vasculopathy.[31–33] Although its pleomorphic effects are widely known, maximizing statin doses is not always possible due to drug interactions and the risk of myopathy and/or renal failure.[34–36] Interestingly, we observed that patients from the progression tertile were younger than those from the least progressive tertile. We believe that a combination of the following 3 factors may confer a greater risk of CAV development in this group: (1) older donor age (45.8 vs 41.9); (2) higher maximal IT during the first month after HTx (0.31 mm vs 0.23 mm; $p = 0.036$); and (3) higher cholesterol and LDL cholesterol levels during the first month after HTx. The traditionally acknowledged risk factors of CAV, such as CMV infection and high-grade rejection episodes, were not predictive of intimal thickness progression in our cohort, possibly due to their low occurrence.

Study limitations

Although it was a dual-center effort, our study comprised a relatively small cohort of patients. This small study size may have affected the significance of relationships assessed, such as CAV risk-factors (e.g., recipient age). Our results should be confirmed in a larger cohort, the data collection of which is ongoing. As OCT evaluation was not performed at the time of HTx, clearly differentiating between donor-transmitted coronary artery disease and de novo progression of CAV was not possible. Due to the additional need for contrast application and the risk of renal function deterioration after OCT, only 1 vessel per patient was examined. Due to limited OCT tissue penetration (1.5 to 3 mm), layered coronary structures, especially the external elastic lamina, were not always visible, thus impacting on the detection of early plaque development. When assessing the relationships between focal wall disease descriptors and ΔIT, the employed parameters (x, y, area) were determined as maximizing the relationship between the developed indices and the increase in intimal thickness at 12 months. Although such an approach lacks physiologic justification,

the existence of a threshold that allows us to study its behavior is of interest, but it requires further research.

In conclusion, we have designed a novel, highly automated 3D image analysis method for analyzing intimal and medial thickness in HTx recipients using coronary OCT. It provides fast, accurate, and highly detailed quantitative data on early CAV changes, which are, in some patients, characterized by significant luminal reduction and intimal thickness progression within the first 12 months after HTx. This diagnostic approach enables such patients to be identified at an early stage, facilitating prompt use of emerging therapeutic methods aimed at preventing further CAV progression.

Disclosure statement

The authors have no conflicts of interest to disclose. This project was supported in part by research grants from the Czech Ministry of Health (16-27465A), MH-CZ-DRO (IKEM-IN 00023001), and the National Institutes of Health (R01-EB004640).

References

1. Ramzy D, Rao V, Brahm J, et al. Cardiac allograft vasculopathy: a review. Can J Surg 2005;48:319-27.
2. Schmauss D, Weis M. Cardiac allograft vasculopathy: recent developments. Circulation 2008;117:2131-41.
3. Cassar Y, Matsuo J, Herrmann J, et al. Coronary atherosclerosis with vulnerable plaque and complicated lesions in transplant recipients: new insight into cardiac allograft vasculopathy by optical coherence tomography. Eur Heart J 2013;34:2610-7.
4. Tsutsui H, Ziada KM, Schoenhagen P, et al. Lumen loss in transplant coronary artery dinase is a biphasic process involving early intimal thickening and late constrictive remodeling: results from a 5-year serial intravascular ultrasound study. Circulation 2001;104:653-7.
5. Matsuo Y, Cassar A, Yoshino S, et al. Attenuation of cardiac allograft vasculopathy by sirolimus: relationship to time interval after heart transplantation. J Heart Lung Transplant 2013;32:784-91.
6. Bilchick KC, Henrikson CA, Skojec D, et al. Treatment of hyperlipidemia in cardiac transplant recipients. Am Heart J 2004;148:200.
7. Dong L, Maehara A, Nazif TM, et al. Optical coherence tomographic evaluation of transplant coronary artery vasculopathy with correlation to cellular rejection. Circ Cardiovasc Interv 2014;7:199-206.
8. Khandhar SJ, Yamamoto H, Teuteberg JJ, et al. Optical coherence tomography for characterization of cardiac allograft vasculopathy after heart transplantation (OCTCAV Study). J Heart Lung Transplant 2013;32:596-602.
9. Park KH, Sun T, Liu Z, et al. Relationship between markers of plaque vulnerability in optical coherence tomography and atherosclerotic progression in adult patients with heart transplantation. J Heart Lung Transplant 2017;36:185-92.
10. Sánchez Lázaro IJ, Almenar Bonet L, Moro López J, et al. Influence of traditional cardiovascular risk factors in the recipient on the development of cardiac allograft vasculopathy after heart transplantation. Transplant Proc 2008;40:3056-7.
11. Zhang H, Abiose AK, Gupta D, et al. Novel indices for left-ventricular dyssynchrony characterization based on highly automated segmentation from real-time 3-D echocardiography. Ultrasound Med Biol 2013;39:72-88.
12. Lee K, Zhang L, Abramoff MD, et al. Fast and memory-efficient LOGISMOS graph search for intraretinal layer segmentation of 3D macular OCT scans. Proc SPIE 20159413: 94133X/1-6.
13. Sun S, Sonka M, Beichel RR. Graph-based IVUS segmentation with efficient computer-aided refinement. IEEE Trans Med Imaging 2013;32:1536-49.
14. Chen Z. Novel quantitative description approaches assessing coronary morphology and development. PhD thesis. Iowa City, IA: University of Iowa; 2016.
15. Clemmensen TS, Holm NR, Eiskjær H, et al. Detection of early changes in the coronary artery microstructure after heart transplantation: A prospective optical coherence tomography study. J Heart Lung Transplant 2018;37:486-95.
16. Mehra MR. Contemporary concepts in prevention and treatment of cardiac allograft vasculopathy. Am J Transplant 2006;6:1248-56.
17. Eisen HJ. Immunosuppression-state-of-the-art: anything new in the pipeline? Curr Opin Organ Transplant 2014;19:500-7.
18. Hou J, Lv H, Jia H, et al. OCT assessment of allograft vasculopathy in heart transplant recipients. JACC Cardiovasc Imaging 2012;5:662-3.
19. Shan P, Dong L, Maehara A, et al. Comparison between cardiac allograft vasculopathy and native coronary atherosclerosis by optical coherence tomography. Am J Cardiol 2016;117:1361-8.
20. Clemmensen TS, Holm NR, Eiskjær H, et al. Layered fibrotic plaques are the predominant component in cardiac allograft vasculopathy: systematic findings and risk stratification by OCT. JACC Cardiovasc Imaging 2017;10:773-84.
21. Cassar A, Matsuo Y, Herrmann J, et al. Coronary atherosclerosis with vulnerable plaque and complicated lesions in transplant recipients: new insight into cardiac allograft vasculopathy by optical coherence tomography. Eur Heart J 2013;34:2610-7.
22. Labarrere CA, Woods JR, Hardin JW, et al. Early prediction of cardiac allograft vasculopathy and heart transplant failure. Am J Transplant 2011;11:528-35.
23. Pethig K, Kofidis T, Heublein B, et al. Impact of vascular branching sites on focal progression of allograft vasculopathy in transplanted hearts. Atherosclerosis 2001;158:155-60.
24. Tambur AR, Pamboukian SV, Costanzo MR, et al. The presence of HLA-directed antibodies after heart transplantation is associated with poor allograft outcome. Transplantation 2005;80:1019.
25. Raichlin E, Edwards BS, Kremers WK, et al. Acute cellular rejection and the subsequent development of allograft vasculopathy after cardiac transplantation. Heart Lung Transplant 2009;28:320.
26. Kapadia SR, Nissen SE, Ziada KM, et al. Impact of lipid abnormalities in development and progression of transplant coronary disease: a serial intravascular ultrasound study. J Am Coll Cardiol 2001;38:206.
27. Fateh-Moghadam S, Bocksch W, Wessely R, et al. Cytomegalovirus infection status predicts progression of heart-transplant vasculopathy. Transplantation 2003;76:1470.
28. Kato T, Chan MC, Gao SZ, et al. Glucose intolerance, as reflected by hemoglobin A1c level, is associated with the incidence and severity of transplant coronary artery disease. J Am Coll Cardiol 2004;43:1034.
29. Ballantyne CM, Radovancevic B, Farmer JA, et al. Hyperlipidemia after heart transplantation: report of a 6-year experience, with treatment recommendations. J Am Coll Cardiol 1992;19:1315.
30. Taylor DO, Thompson JA, Hastillo A, et al. Hyperlipidemia after clinical heart transplantation. J Heart Transplant 1989;8:209.
31. Kobashigawa JA, Katznelson S, Laks H, et al. Effect of pravastatin on outcomes after cardiac transplantation. N Engl J Med 1995;333:621.
32. Kwak B, Mulhaupt F, Myit S, et al. Statins as a newly recognized type of immunomodulator. Nat Med 2000;6:1399.
33. Weis M, Pehlivanli S, Meiser BM, et al. Simvastatin treatment is associated with improvement in coronary endothelial function and decreased cytokine activation in patients after heart transplantation. J Am Coll Cardiol 2001;38:814.
34. Vanhaecke J, van Cleemput J, van Lierde J, et al. Safety and efficacy of low dose simvastatin in cardiac transplant recipients treated with cyclosporine. Transplantation 1994;58:42.
35. Rodríguez JA, Crespo-Leiro MG, Paniagua MJ, et al. Rhabdomyolysis in heart transplant patients on HMG-CoA reductase inhibitors and cyclosporine. Transplant Proc 1999;31:2522-3.
36. Szyguła-Jurkiewicz B, Szczurek W, Zembala M. The role of statins in patients after heart transplantation. Kardiochir Torakochirurgia Pol 2015;12:42-7.